International Journal of Scientific Engineering and Applied Science (IJSEAS) – Volume-2, Issue-4,April 2016
ISSN: 2395-3470
www.ijseas.com

Prediction of Instantaneous Burning Rate of Solid Propellant for a Solid Rocket Motor

E. Nnali-uroh[1], K.F. Oyedeko[2], Prince Anyaba [3]

[1, 2] Department of Chemical and Polymer Engineering, Lagos State University, Lagos, Nigeria. [2]
[1]nnali_emma@yahoo.com, [2]kfkoyedeko@yahoo.com,

[3] Center for space transport and propulsion Epe, Lagos, Nigeria.

ABSTRACT

The starting point in the characterisation of solid propellant is to measure the burn time, pressure and thrust generated by the propellant in the combustion chamber. From this a model to predict instantaneous burning rate is developed using thrust which is related to burning rate at steady state. A nonlinear ordinary differential equation obtained from the model formulated was solved using Euler method to obtain the regression distance and computed in Microsoft Excel Spread Sheet by applying features like goal to ensure that final regression distance was equal to the web thickness of the propellant before ignition. The average burn rate estimated using trapezium rule to obtain the area under a thrust – time curve at steady state was 8.85mm/s for a pressure range of 104 – 160 PSI. The pressure coefficient (a) and exponent (n) were also estimated as a = 10.40 and n = 0.440 by plotting the rising instantaneous burning rate versus pressure in excel spread sheet and fitting a power function using trend line option. The results were validated to 95.5% accuracy using CP-Technology characterisation software and normal calculations. The percentage of accuracy was reasonable enough when validated. The obtained model can be used to characterise any other type of solid propellant by varying the propellant properties at any time.

Key words: Burning rate, Combustion chamber, Pressure, Solid propellant, Thrust.

1. Introduction

The rocket motor designer must have a good understanding of the variation of propellant burning rate with both pressure and temperature in order to produce an efficient design and minimize design iterations during development. It is a well-known fact that the burning rate deduced from test firings of full-scale motors sometimes differs from that measured in strand burner. (Fry 2001). This difference is typically only a few percent but this may be sufficient to cause motor performance to lie outside the required limits and force a change in propellant formulation, motor grain design or nozzle throat diameter with associated cost and schedule penalties. Difficulties may also arise when burning rate data for a given propellant formulation is passed across national boundaries as in technology exchange programs or even when passed from company to company within the same country. If the size and type of device used to generate the baseline data is not fully taken into account then the data cannot be correctly interpreted and errors due to scale-up may result (Fry 2001).

Solid rocket propellants are the power behind propulsion of all modern missiles and most launch vehicles. Rocket propellant is fired on the ground in a rocket motor with known throat diameter for realisation of pre-specified pressure and thrust inside rocket motor chamber. The performance prediction of a solid propellant requires

internal ballistic calculations and in most of the cases, mass conservation is imposed to estimate various ballistic parameters. The applicability of empirical power law (known as Saint Roberts law) for relating burning rate with generated pressure has two important performance parameters namely pressure index (n) and burning rate coefficient (a). It is an empirical relationship showing dependence of burning rate on pressure in rocket motor chamber during motor operation and is used for performance prediction of rocket motors. Burning rate (r) and pressure in rocket motor chamber (P) are measurable parameters, but pressure coefficient (a) and pressure exponent (n) are empirical constants which vary with propellant and operating conditions (Hinanshu 2009). The burning rate of a solid propellant may be defined as the velocity with which the burning surface recede in a direction perpendicular to the original surface; the rate is usually measured in millimetre per seconds. The propellant burning rate is influenced by certain factors, such as combustion chamber pressure, initial temperature of the propellant grain, velocity of the combustion gasses flowing parallel to the burning surface and local static pressure, (Nakka, 2013).

All propellants are made up of two parts: Oxidizer and Fuel (or reducer). An oxidizer is a component that produces oxygen for reaction with the fuel. Fuel reacts with the oxygen to produces gas for propulsion. The fuel used in space vehicles is very much different from the normal fuel in respect to the following properties, (MFC Propulsion, 2013).

Depending on the physical state of fuel and oxidiser, propellants are classified as: Solid propellants, Liquid propellants, Hybrid propellants. (Space Travel Guide, 2014)

The shape of the fuel block for a rocket is chosen for the particular type of mission it will perform. Since the combustion of the block progresses from its free surface as this surface grows, geometrical considerations determine whether the thrust increases, decreases or stays constant. (Braeunig, 2012)

The initial grain geometry of a solid propellant strictly depends on the propulsive mission. The following nomenclature is used: Grain configuration, End-burning grain, Cylindrical grain:, Perforation, Inhibitor, Restricted surface, Sliver: unburned propellant remaining at the time of web burnout. To accomplish this task, a cylindrical bates grain configuration was used because of the expected burn duration of the propellant and the progressive thrust profile of the configuration. (Sutton, 1992)

Over the years, several modifications of this basic setup for solid strands have been proposed. In the most common modification, the whole apparatus can be placed in a thermally controlled environment capable of producing the desired initial temperature range. In another version, called window strand burner, the burner is equipped with optical windows allowing optical recording of the burning processes (still photography, movie camera, video camera, etc. both in the visible and infrared ranges). At Thiokol/Huntsville, a bomb holding three strands was used, (Zanotti *et al* 1992). All configurations are easy and quick to operate, use a minor amount of propellant, and require little instrumentation. Thus, the strand burner method is widely used.

The strand is ignited at the top by a hot wire, and the time taken for burning to pass from the first to the second fuse wire is accurately measured. It is usual to take several measurements at each pressure, (Huggett, 1960). The burning surface should remain planar and normal to the strand axis.

For about 50 years, the industry standard apparatus for the measurements of linear burning rates was the Crawford bomb (Crawford, 1947). This method which is very quick, simple and economical is particularly suitable for exploring new propellant compositions or performing quality control of established compositions

But the technique of vented vessels is still used today for other purposes such as interrupted burning to examine the conditions of the propellant charge during combustion, (Barrere et al 1960). Several closed vessel configurations are currently available to obtain the burning rate of the propellant from experimental pressure records in time. This is not a direct measurement and the overall approach is a laborious process requiring a number of assumptions, but the method is still used today for very high pressure combustion (gun propellants), (Williams, 1985, Holzmann, 1969, Zarko and Kuo,1994)

An alternative technique to assess performances of gun propellants in particular is to measure the heat of explosion in some type of calorimeter. This is a sensitive and quick method, derived from chemistry, capable of detecting any important changes or gross error in chemical composition. But it is useful in rocket propulsion only if for the given propellant the rate of burning is directly related to the heat of explosion which is not commonly the case, (Juhasz and Price 2004, Boggs, 1992). By changing the shape and size of the perforation in the propellant, the rate and duration of burning can be controlled and thus controlling the thrust. The more the thrust required, the larger the perforation but the fuel will burn for a smaller time. The lesser the thrust required, the smaller the perforation but the fuel will burn for a very long time. The burning period and the thrust depend upon the type of perforation in the fuel, (Space Travel Guide, 2014). Several of these techniques (in particular microwaves and ultrasonic) are also apt to measure transient burning rates; in addition, the acoustic emission technique is apt to provide information as to the burning rate non uniformity (due to localized and intermittent burning rate variations), (Eisenreich *et al* 1987, Tauzia and Lamarque, 1998, Strand and Reed, 1980, Caveny *et al* 1976, Mihlfelth *et al* 1972, Yang and Ramanos 1990,). An accuracy of about: I per cent in instantaneous burn rate measurements and reproducibility of results have been demonstrated by applying ultrasonic technique, (Cauty 2000).

This work predicts the instantaneous burning rate of solid propellant by formulating the model and solving the model through transforming the thrust terms to pressure before simulating. This is done by using a load cell for the characterisation of a hollow cylindrical bates grain solid propellant at a pressure range of 104 - 160 PSI and solid propellant known as MOD-KNSU,

2. Methodology

To accomplish this task, the following instruments and equipment were used, DC power source, Instrumentation panel, Digital launch control system, Laptop, Safety indicator, Connecting cables, Propellant, Igniter, Combustion chamber, Load cell

2.1 Model formulation

This was done in three parts, it involves

A. Model development for pressure builds up inside the combustion chamber.
B. Modeling the Burning Surface Area of Propellant, Ab as a function of Surface Regression Distance, s(t)

C. The specific impulse

2.2 Model development for pressure builds up inside the combustion chamber.

Assumptions

i. The combustion chamber is assumed to be a ′perfectly well-mixed′.
ii. The combustion gases follow the ideal gas law.
iii. The solid propellant burning follows the St. Robert's burning law. The burning occurs only at the internal and the side surfaces of the solid propellant.
iv. Heat transfer was negligible.
v. The mass added by the burning propellant is at the adiabatic flame temperature of the propellant at the specified gradient.
vi. Frictional forces between the propellant surface and combustion gas is negligible.
vii. Erosive burning was not considered.

2.3 Modelling Pressure Build-up Inside the Thrust Chamber During Propellant Grain Deflagration

From the Principle of conservation of mass

Rate of combustion product generation = rate of consumption of the propellant grain

$$\dot{m}g = A_b \rho_p r \tag{1}$$

Assuming ideal case were only gaseous product result (no solids or liquid) where $\dot{m}g$ = rate of combustion product generation, A_b = grain burning area , ρ_p = propellant density, r = propellant burn rate

The rate at which gas is stored in the combustion chamber is given by:

$$\frac{dm_s}{dt} = \frac{d}{dt}\left(\rho_o V_o\right) \tag{2}$$

Where ρ_o = instantaneous gas density, V_o = instantaneous chamber volume (free volume within the chamber)

$$\frac{dm_s}{dt} = \rho_o \frac{dV_o}{dt} + V_o \frac{d\rho_o}{dt} \tag{3}$$

The change in gas volume with respect to time is equal to the change in volume due to the propellant consumption, i.e

$$\frac{dV_o}{dt} = A_b r \tag{4}$$

$$\frac{dm_s}{dt} = \rho_o A_b r + V_o \frac{d\rho_o}{dt} \tag{5}$$

The principle of mass conservation requires the balance between mass generation rate and the sum of the rates at which mass storage in the chamber and outflow through the nozzle:

$$\dot{mg} = \frac{dm_s}{dt} + \dot{m}_n \tag{6}$$

where $\dot{m}_n$ = mass flow rate through the nozzle

substituting Eq. (1) and Eq. (5) into Eq. (6) gives

$$A_b \rho_p r = \rho_o A_b r + V_o \frac{d\rho_o}{dt} + \dot{m}_n \tag{7}$$

For $\dot{m}_n$ = mass flow rate through the nozzle = $\frac{Av}{V}$ (8)

where A = nozzle cross sectional area, v = Velocity of the flow , V = Specific volume

For velocity of the flow at the throat, (Principle of conservation of linear momentum)

$$h_1 - h_2 = \frac{1}{2}\left(v_2{}^2 - v_1{}^2\right) = C_p\left(T_1 - T_2\right) \tag{9}$$

where h = enthalpy change of the fluid, C_p = heat capacity of the fluid, T = fluid temperature

Using $k = \frac{C_p}{C_v}$ and $R = C_p - C_v$ gives

$$\therefore\ C_p = \frac{kR}{k-1} \tag{10}$$

where R = specific gas constant, k = ratio of specific heat or isentropic exponent,

Cp= specific heat capacity

From Eq. (9)

$$v_2 = \sqrt{2C_p(T_1 - T_2) + v_1^2} \tag{11}$$

Substituting Eq. (10) into Eq. (11) gives

$$v_2 = \sqrt{\frac{2kR}{k-1}(T_1 - T_2) + v_1^2} \tag{12}$$

For isentropic flow process

$$\frac{T_1}{T_2} = \left(\frac{P_1}{P_2}\right)^{\frac{k-1}{k}} = \left(\frac{V_2}{V_1}\right)^{\frac{K-1}{}} \tag{13}$$

$$T_2 = T_1\left(\frac{P_2}{P_1}\right)^{\frac{K-1}{K}} \tag{14}$$

Substituting Eq. (14) into Eq. (12) gives

$$v_2 = \sqrt{\frac{2kR}{k-1}\left(T_1 - T_1\left(\frac{P_2}{P_1}\right)^{\frac{k-1}{k}}\right) + v_1^2} \tag{15}$$

For adiabatic process, $v_1 = 0$ and $v_2 = v$

$$v = \sqrt{\frac{2kR}{k-1}T_1\left(1 - \frac{P_2}{P_1}\right)^{\frac{k-1}{k}}} \tag{16}$$

From Eq. (13)

$$\left(\frac{P_1}{P_2}\right)^{\frac{k-1}{k}} = \frac{T_1}{T_2} = T_1 \times \frac{1}{T_2} \tag{17}$$

But $C_P(T_1 - T_2) = \frac{1}{2}\left(v_2^2 - v_1^2\right)$

When $v_1 = 0$, $v_2 = v$

$$T_1 = \frac{v^2}{2C_p} + T_2 \tag{18}$$

Substituting Eq. (18) into Eq. (17) gives

$$\left(\frac{P_1}{P_2}\right)^{\frac{k-1}{k}} = 1 + \left(\frac{k-1}{2}\right)\frac{v^2}{kRT_2}$$

Mach number $M = \frac{v}{a^*}$ and $a^* = \sqrt{kRT}$

Where a^* = local sonic velocity

$$M = \frac{v}{\sqrt{kRT}}, \quad M^2 = \frac{v^2}{kRT}$$

$$\left(\frac{P_1}{P_2}\right)^{\frac{k-1}{k}} = 1 + \frac{k-1}{2}M^2 \quad (M = 1 \text{ at the throat})$$

$$\left(\frac{P_1}{P_2}\right)^{\frac{k-1}{k}} = \left(\frac{k+1}{2}\right)^{\frac{k}{k-1}}$$

Therefore,

$$\frac{P_2}{P_1} = \left(\frac{2}{k+1}\right)^{\frac{k}{k-1}} \tag{19}$$

Substituting Eq. (19) into Eq. (16) gives

$$v = \sqrt{\frac{2kRT_1}{k-1}\left(1 - \left(\frac{2}{k+1}\right)^{\frac{k}{k-1}}\right)^{\frac{k-1}{k}}}$$

$$v = \sqrt{\frac{2kRT_1}{k-1}\left(\frac{k-1}{k+1}\right)} = \sqrt{\frac{2kRT_1}{k+1}} \tag{20}$$

From the thermodynamic equation of Eq. (9),

$$\frac{1}{2}\left(v_2{}^2 - v_1{}^2\right) = C_p\left(T_1 - T_2\right)$$

When $v_1 = 0$, $v_2 = v$ gives

, $$\frac{v^2}{2C_p} = T_1 - T_2$$

$$T_1 = T_2 + \frac{v^2}{2C_p} \tag{21}$$

Combing Eq. (13) and Eq. (21) gives

$$V_2 = V_1\left(1 + \frac{v^2}{2C_pT_2}\right)^{\frac{1}{k-1}}$$

Using $C_p = \frac{kR}{k-1}$ and rearranging to gives

$$V_2 = V_1\left(1 + \left(\frac{k-1}{2}\right)\left(\frac{v^2}{kRT_2}\right)\right)^{\frac{1}{k-1}}$$

But $M^2 = \frac{v^2}{kRT_2} = 1$

$$V_2 = V_1\left(\frac{2+k-1}{2}\right)^{\frac{1}{k-1}} = V_1\left(\frac{k+1}{2}\right)^{\frac{1}{k-1}} \tag{22}$$

Substitutimg into Eq. (8)

$$\dot{m}_n = \frac{A\sqrt{\frac{2kRT}{k+1}}}{V_1\left(\frac{k+1}{2}\right)^{\frac{1}{k-1}}} \tag{23}$$

From ideal gas equation

$$V = \frac{RT}{P} \tag{24}$$

Substituting Eq. (24) into Eq. (23) gives

$$\dot{m}_n = \frac{A\sqrt{\frac{2kRT}{k+1}}}{\frac{RT}{P}\left(\frac{k+1}{2}\right)^{\frac{1}{k-1}}}$$

Reduce to

$$\dot{m}_n = P_o A\sqrt{\frac{k}{RT}\left(\frac{2}{k+1}\right)^{\frac{k+1}{k-1}}} \tag{25}$$

Substituting Eq. (25) into Eq. (7)) gives

$$A_b\rho_p r = \rho_o A_b r + V_o\frac{d\rho_o}{dt} + P_o A\sqrt{\frac{k}{RT}\left(\frac{2}{k+1}\right)^{\frac{k+1}{k-1}}} \tag{26}$$

But $r = a\cdot P_o^{\,n}$ (Saint Robert's law) (Fry and Hopkins, 2001) (27)

r = propellant burn rate, a = burn rate coefficient, n = pressure exponent

Substituting Eq. (27) into Eq. (26)

$$A_b\rho_p aP_o^{\,n} = A_b\rho_o aP_o^{\,n} + V_o\frac{d\rho_o}{dt} + P_o A\sqrt{\frac{k}{RT_o}\left(\frac{2}{k+1}\right)^{\frac{k+1}{k-1}}}$$

But $PV = nRT$; $\rho = \frac{1}{V} = \frac{P}{RT}$

$$\frac{d\rho_o}{dt} = \frac{dP}{dt}\cdot\frac{1}{RT} = \frac{1}{RT}\frac{dP}{dt} \tag{28}$$

$$\frac{V_o dP_o}{RT_O dt} = A_b\rho_p aP_O^{\,n} - A_b\rho_o aP_o^{\,n} - P_o A\sqrt{\frac{k}{RT_O}\left(\frac{2}{K+1}\right)^{\frac{K+1}{K-1}}}$$

At steady state when the outflow of combustion gases is in equilibrium with the production of gases from propellant combustion $\frac{dP_o}{dt} = 0$ and because $\rho_p \gg \rho_o$ so ρ_o is dropped out.

$$0 = A_b \rho_p a P_o^{\,n} - P_o A \sqrt{\frac{k}{RT_o}\left(\frac{2}{k+1}\right)^{\frac{k+1}{k-1}}}$$

$$P_o = \left(\frac{A_b}{A}\right)\left(\rho_p a P_o^{\,n}\right)\sqrt{\frac{RT_o}{k\left(\frac{2}{k+1}\right)^{\frac{k+1}{k-1}}}} \tag{29}$$

using $k = \frac{A_b}{A}$, $r = aP_o^{\,n}$, $C^* = \sqrt{\frac{RT_o}{k\left(\frac{2}{k+1}\right)^{\frac{k+1}{k-1}}}}$ ` giving

$$P_o = k.\rho_p.r.C^*$$

$$P_c = k_n r \rho_p C^*$$

$$P_c = k_n r \rho_p C^* \tag{30}$$

Eq. (30) is the steady state pressure which needs to be to be transformed to relate burning rate and thrust.

$$I_{sp} = \frac{F}{g\,\dot{m}_t} \tag{31}$$

$$\dot{m}_t = \frac{P_c A_t}{C^*} \tag{32}$$

Substituting Eq. (30) into Eq. (32)

$$\dot{m}_t = k_n \rho_p r A_t \tag{33}$$

using $k_n = \frac{A_b}{A_t}$ gives

$$m_t = \dot{A}_b \rho_p r \tag{34}$$

Rearranging Eq. (31) and equating with Eq. (34) gives

Equating Eq. (36) and Eq. (37)

$$r = \frac{F}{A_b \rho_p I_{sp} g} \tag{35}$$

But $r = \frac{ds}{dt}$

$$\frac{ds}{dt} = \frac{F(t)}{A_{b(s)} \rho_p I_{sp} g} \tag{36}$$

Eq. (36) is the burning rate – thrust relationship with burning surface area dependent on regression distance and specific impulse (Isp) while the other terms (g and rho p) are constant.

$$s_{n+1} = s_n + \Delta t \bullet \left(\frac{ds}{dt} \right)\Big|_{t_n} \tag{37}$$

Since the pressure coefficient and exponent can be obtained from a plot of burning rate and pressure, a relationship between pressure and thrust needs to be established as shown below

$$C_f = \frac{F}{P_c * A_t} \tag{38}$$

From Eqn 31, Eqn 32 and Eqn 38

$$P_c = \frac{F}{A_t * C_f} \tag{39}$$

Equation (39) holds when

$$C^* = \frac{I_{sp} * g}{C_f}$$

2.4 Modeling the Burning Surface Area of Propellant, A_b as a function of Surface Regression Distance, s(t)

Outer surface area of a hollow cylinder = $\Pi * D * L$ = 0 (since the outer surface is inhibited. See appendix C for diagrams of area of consideration)

Core surface area = $\Pi * d * L$, Surface area of the ends = $2\Pi\left(\frac{D^2 + d^2}{4}\right)$

The total surface area of an inhibited hollow cylindrical grain is given as

$$A_b = N * \Pi * \left(\frac{D^2 - d^2}{2} \right) + \Pi * d * L \tag{40}$$

N = total number of bates grain. But, $d = d_o + 2s$, $L = L_o - 2s$

Therefore,

$$A_b = \frac{1}{2}\pi\left(D^2 - (d_o + 2s)^2\right) + \pi(d_0 + 2s)(L_o - 2s) \tag{41}$$

For inhibited surface,

$$A_b = N\left(\frac{1}{2}\pi\left(D^2 - (d_o + 2s)^2\right) + \pi(d_o + 2s)(L_o - 2s)\right) \tag{42}$$

$$A_b = N\left(\pi\left(\frac{1}{2}\left(D^2 - (d_o + 2s)^2\right) + (d_o + 2s)(L_o - 2s)\right)\right) \tag{43}$$

Eq. (43) is the burning surface area surface inhibited grain as a function of regression distance.

2.5 The specific impulse

This was obtained from the following relationships

$$I_{sp} = \frac{I_t}{m_p * g} \tag{44}$$

$$I_t = \int_t^{tb} F dt \tag{45}$$

2.6 Solution Technique

A nonlinear ordinary differential equation formulated for burning rate as shown in Eq. (36) was solved using Euler method to obtain a predicted burning distance, (s). This is expressed mathematically as Eq. (37).

2.7 Procedure Prior to Testing

The MOD_KNSU propellant was prepared, casted and dried followed by insertion into the combustion chamber, the igniter was inserted and the complete system was closed to ensure there was no opening except through the nozzle. The rocket motor was placed on the load cell after the later has been calibrated. Signal was sent from a remote controller to the instrumentation panel to activate the launch command which sends an electric impulse to an igniter to initiate the combustion process. During the

combustion process, the thrust (Force) produced was sensed as an electrical signal by the load cell and recorded by the data acquisition module which serves as an intermediary between the load cell and the laptop where this signals are collected as data for further processing.

3. Results and Discussion

The model formulated was solved and simulated with Microsoft Excel Spread Sheet to generate instantaneous burning rates for MOD_KNSU solid propellant. The results of this simulation are presented below.

3.1 Total Impulse

The total impulse was obtained from Eq. (45) by taking the area under the curve in Fig. 1 using trapezium rule. This was done by setting out the Excel spread sheet as shown in Table 1 below.

From the Table 1, a plot of thrust versus time was made to generate a thrust-time profile for the solid propellant (Fig.1). Using trapezium rule, the total impulse of the propellant was estimated as 3780.0775Ns. This value was used to estimate the specific impulse according to Eq. (44) of the propellant which is given as total impulse divided by total mass of propellant multiplied by acceleration due to gravity as 96.3seconds.

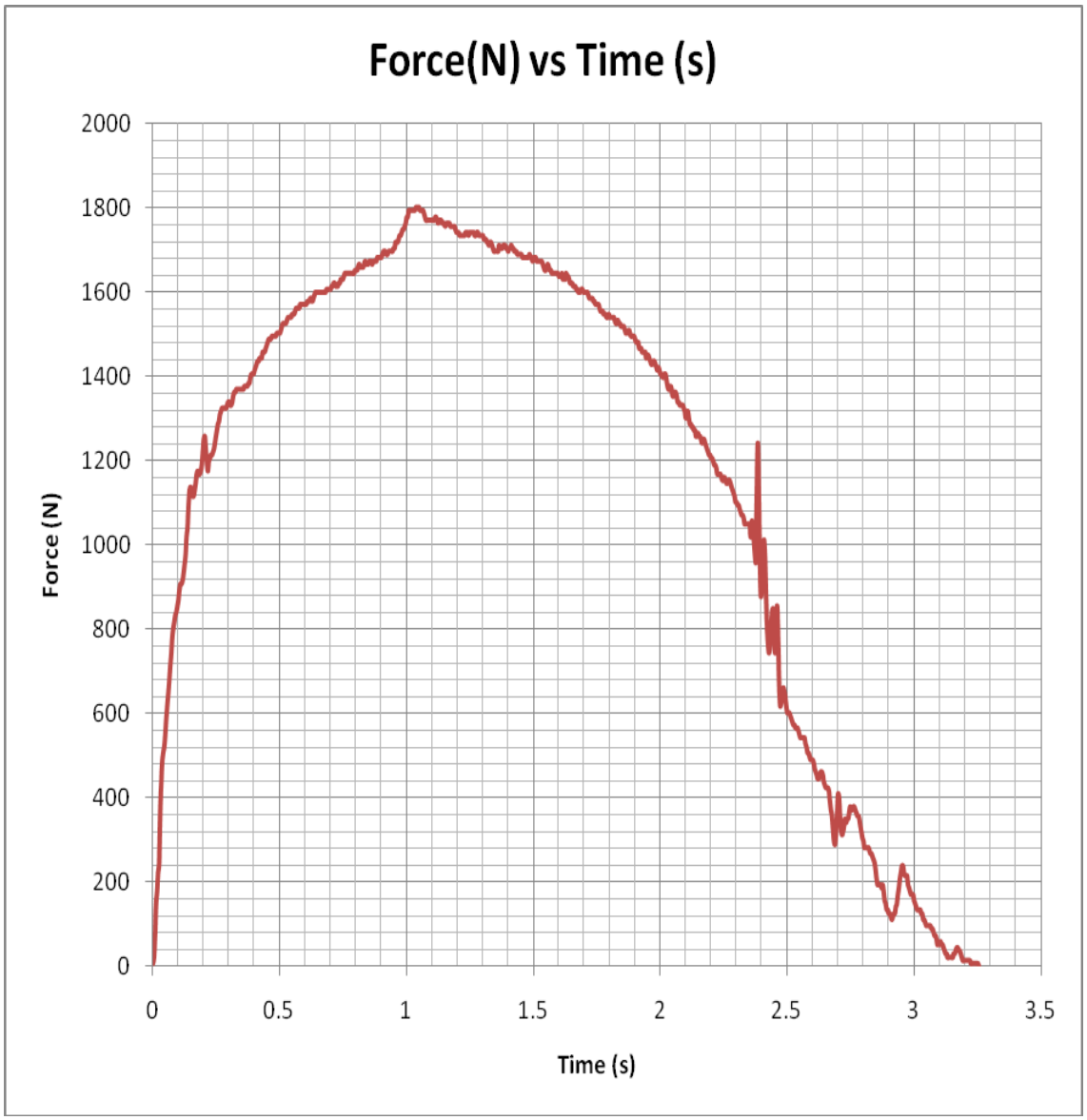

Fig. 1 Thrust – Time Profile.

Table 1. Spreadsheet set up for total impulse estimation.

Column A, The propellant burn time, Column B Experimental thrust reading from the load cell, Column C The actual thrust produced by the propellant during combustion, Column D The total impulse of the propellant (Eq. 21), Samples per sec. = 256/1 initial Cell Thrust =170.64 Isp = 96.332249s

A	B	C	D
Time (sec)	F(N)expt	F(N)act.	Impulse(Ns)
0	177.83	7.19	0
0.004	192.2	21.56	0.0575
0.008	244.29	73.65	0.24792
0.012	319.73	149.09	0.6934
0.016	348.47	177.83	1.34724
0.02	393.38	222.74	2.14838
0.024	416.73	246.09	3.08604
0.028	528.1	357.46	4.29314
0.032	601.75	431.11	5.87028
0.036	653.84	483.2	7.6989
0.04	677.19	506.55	9.6784
0.044	691.56	520.92	11.73334
0.048	720.3	549.66	13.8745
0.052	758.02	587.38	16.14858
0.056	788.56	617.92	18.55918
0.06	817.3	646.66	21.08834
0.064	847.84	677.2	23.73606
0.068	883.76	713.12	26.5167
0.072	914.3	743.66	29.43026
0.076	952.02	781.38	32.48034
0.08	973.57	802.93	35.64896
0.084	987.94	817.3	38.88942
0.088	1004.1	833.46	42.19094
0.092	1011.3	840.66	45.53918
0.096	1025.7	855.06	48.93062

To predict the instantaneous burning rate from the generated thrust, the excel spread sheet was set up as shown in Table 2 below.

Table 2. Spread sheet set up for propellant burning rate determination

initial Cell Thrust = 170.64 N= 3 , do = 0.038m , Dt = 0.036m

D= 0.105m Lo= 0.13m , At = 0.001017876 m2 N g= 9.81m/s2 cf= 1.2

c*=787.2525m/s ρp=1896 kg/m3 Δt = 0.004s wo=0.0335m Isp = 96.3s

A Time(s)	B F(N)expt	C F(N)	D Ab(m^2)	E s(m)	F s(mm)	G Δs/Δt(m/s)	H Δs/Δt(mm/s)	I P_c(N/m^2)	J P_c(MPa)	K Δs/Δt(m/s)P	L Rb
0	1345.4	1174.76	0.0958	0.01188	11.878	0.006845	6.8447971	961774	0.96177	0.0068448	0
0.004	1368.8	1198.16	0.0958	0.01191	11.906	0.006982	6.9817909	980932	0.98093	0.00698179	0.132441
0.008	1375.9	1205.26	0.0958	0.01193	11.934	0.007024	7.0238393	986744	0.98674	0.00702384	0.173147
0.012	1383.1	1212.46	0.0958	0.01196	11.962	0.007066	7.0664893	992639	0.99264	0.00706649	0.214675
0.016	1383.1	1212.46	0.0958	0.01199	11.99	0.007067	7.0671912	992639	0.99264	0.00706719	0.214675
0.02	1390.3	1219.66	0.0958	0.01202	12.018	0.00711	7.1098715	998534	0.99853	0.00710987	0.256460
0.024	1397.5	1226.86	0.0958	0.01205	12.047	0.007153	7.1525716	1004428	1.00443	0.00715257	0.298496
0.028	1411.9	1241.26	0.0958	0.01208	12.075	0.007237	7.2372719	1016217	1.01622	0.00723727	0.383318
0.032	1428	1257.36	0.0957	0.0121	12.104	0.007332	7.3319189	1029398	1.0294	0.00733192	0.479337
0.036	1442.4	1271.76	0.0957	0.01213	12.134	0.007417	7.4166896	1041188	1.04119	0.00741669	0.566275
0.04	1456.8	1286.16	0.0957	0.01216	12.163	0.007501	7.5014958	1052977	1.05298	0.0075015	0.654212

Columns A – C are as defined above.

Column D-Inhibited bate grain burning surface area (Eq. 43)

Column E The regression distance, the initial value was assumed. Using goal seek tool, the final value of 0.0335 was obtained which corresponds to the propellant web thickness before ignition (Eq. 37)

Column F Regression distance in millimetre (mm)

Column G Burn rate from thrust generated, this excludes the ignition and extinction period in meter per second (m/s) (Eq. 36)

Column H Burn rate from thrust generated, this excludes the ignition and extinction period in meter per second (mm/s)

Column I Pressure estimated from pressure – thrust relationship (N/m^2) (Eq. 39)

Column J Pressure estimated from pressure – thrust relationship (MPa)

Column K Burn rate based on estimated pressure

Column L Application of trapezium rule to estimate the burning rate as an area under the curve of the plot of thrust (column C) versus time (column A) with the exclusion of start-up and tail off period as shown in Fig. 2 below

The normal practice is to determine pressure dependent burning rate and this was done on column M148 with a value of 3.623mm/s.

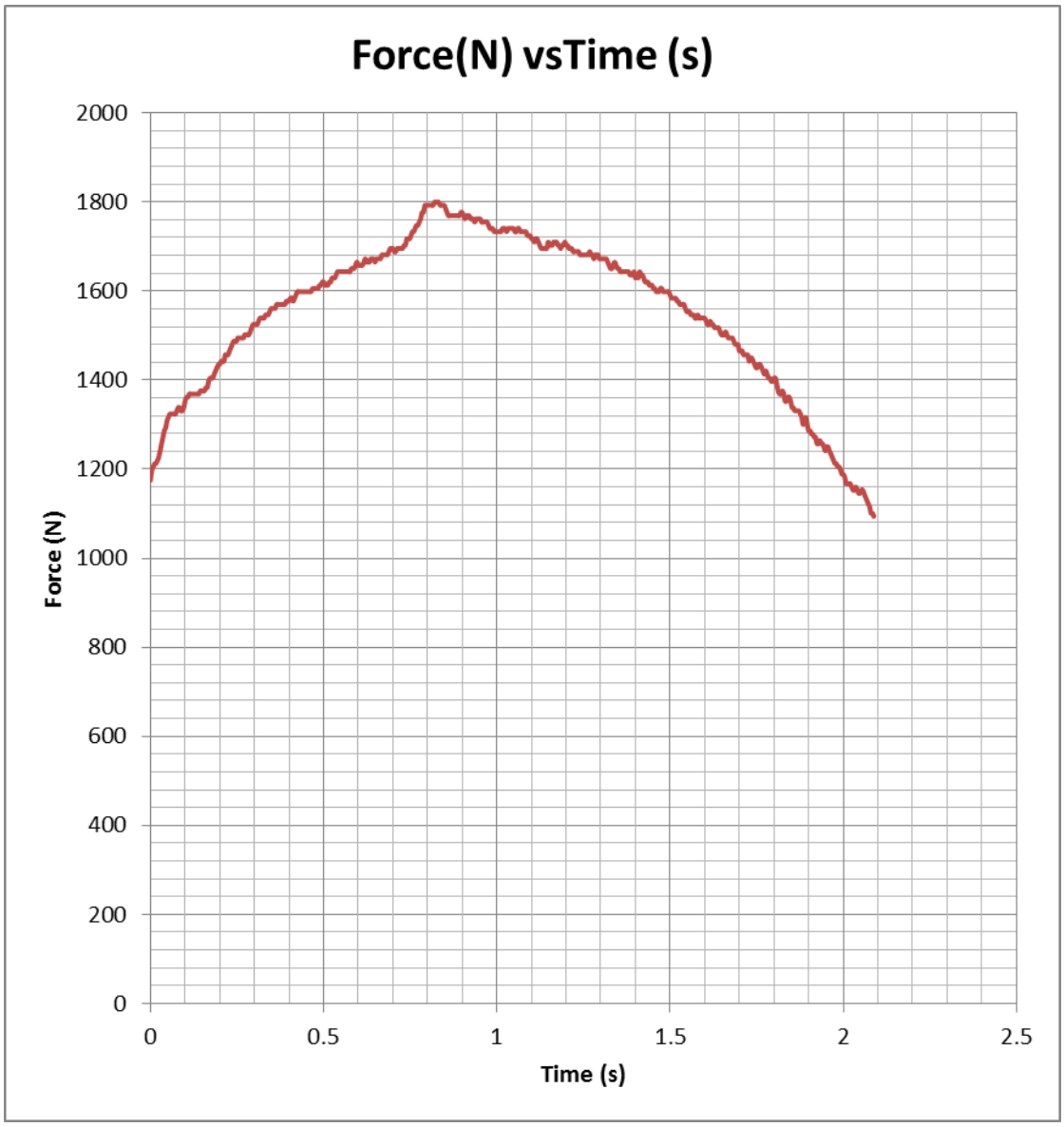

Fig. 2 Thrust –time profile for steady state (excluding start-up and tail – off)

3.2 Pressure Coefficient (a) and Exponent (n)

The values for these constants were obtained by plotting the values of burn rate (column H) against pressure (in MPa, column J), the plot is shown in Fig. 3 below. The values of a= 10.40 and n = 0.440 were obtained by fitting a power function on the plot from trend line option in Excel Spread Sheet. From literatures, the value of n for the kind of propellant used in this report is within the range of $0.2<n<0.8$. From the result of the task, the value of n (0.440) obtained was within the said range. The result shows that at least 98.5% of the data was captured in the plot and that also validates the result statistically.

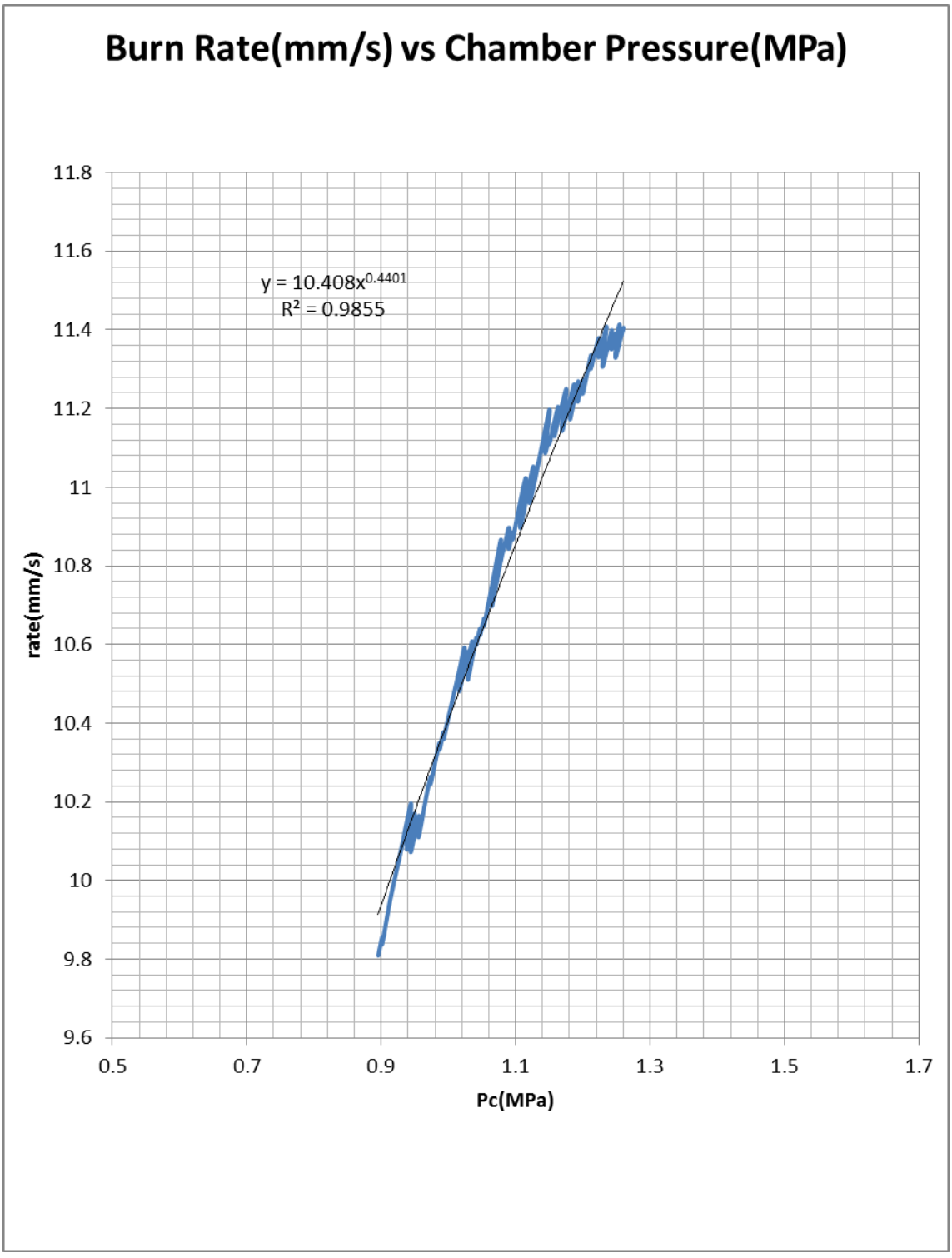

Fig. 3 Plot of burning rate versus pressure

3.4 Result Validation

To validate the results of Burn rate analysis, the pressure range was inputted into CP Technology software called CHEM – Propellant thermochemistry. The details are in Table 2. Also the maximum thrust read by the load cell, the burning surface area of inhibited grain (different from instantaneous burning surface area), the propellant density,

specific impulse with acceleration due to gravity were applied in the formula for estimating burning rate in column H, the result obtained was 3.724mm/s compared to 3.623mm/s obtained by the model. The differences for these three parameters were found, the average percentage accuracy was 95.5%.

Table 3. Validation of Burn Rate Analysis Results

S/N	Parameter	Model	CP-Tech.	Difference
1	Specific impulse (Isp) (s)	96.3	106.3	10
2	Characteristic exhaust velocity (C*) (m/s)	787.3	797.4	10.1

Table 4. Summary of Estimated values from model at a pressure range of 104.26 – 158.21 PSI

S/N	PARAMETERS	VALUES
1	Total impulse (Ns)	3780.0775
2	Specific impulse (s)	96.3
3	Burning rate (mm/s)	8.85
4	A	10.4
5	N	0.440
6	C* (m/s)	787.3

4. Conclusion

The burning rate of a propellant and how it changes under various conditions is of fundamental importance in the successful design of a solid rocket motor. The rate of regression, typically measured in millimetre per second is termed burning rate. This rate can differ significantly for different propellants or for one particular propellant depending on

various operating conditions as well as formulation. Accuracy of solid rocket thrust-time prediction has become increasingly more important in solid rocket design. One of the most significant variables in this prediction is the propellant burning rate.

From the model, it was observed that the burning rate of the propellant was dependent on the burning surface area of the propellant which was derived as a function of regression distance and the regression distance was obtained numerically using Euler method. The average burning rate was obtained as 8.85mm/s from the area under the thrust – time profile for a steady state condition using trapezium rule. Since burning rate s is pressure dependent, the thrust obtained from the experiment was transformed into pressure by thrust – pressure relationship. From the plot of instantaneous burning rate versus pressure, the pressure coefficient and exponent were obtained as 10.40 and 0.440.

From literatures, the value of n for the kind of propellant used in this report is within the range of $0.2<n<0.8$. From the result of the task, the value of n (0.440) obtained was within the said range. The result shows that at least 98.5% of the data was captured in the plot and that also validates the result statistically.

This task has been able to formulate a model which was solved by Euler method and simulated in a Microsoft excel spread sheet for estimating the burning rate, pressure exponent and coefficient for MOD_KNSU solid propellant. This process can also be adopted in characterising any solid propellant.

REFERENCE

M. Barrere, A. Jaumotte, B. Fraeijs De Veubeke and J. Vandenkerchove Rocket propulsion, Elsevier publishing company, Amsterdam, Netherlands, 1960.

T.L. Boggs. ‘’Experimental Diagnostics in Combustion of Solids’’. AIAA, Washington DC USA, 1992, pp. 129-151.

R.A. Braeunig. Rocket and space Technology, Rocket propulsion. 2012

B.L.Jr. Crawford. ‘’Direct Determination of Burning rates of Propellant Powders’’, Analytical chemistry,1947, pp. 630-633.

F. Cauty. ‘’Ultrasonic Method Applied to Full-Scale Solid Rocket Motors’’, Journal of Propulsion and Power 16(3), 2000, pp. 523-528.

L.H. Caveny. A. J. Saber, and M. Summerfield. ‘’Propellant combustion and burning rate uniformity identified by ultrasonic Acoustic Emissions’’, AIAA, Washington DC, 1976, pp. 76-696.

N. Eisenreich, H.P. Kugler, and F. Sinn. An Optical System for Measuring Burning Rates of Solid Propellants, Explosives and Pyrotechnics. 1987

R.S. Fry. ‘’Solid propellant Test Motor Scaling’’, CPTR 73, Maryland, 21044-3204, CPIA, pp 1, September 2001.

R.S. Fry and J. Hopkins. ‘’Evaluation of methods for solid propellant burning rate measurement’’, NATO RTO Advissory Reprot, NATO RTO AVT Working group 016. August 2001.

C. Huggett. Solid propellant Rockets No 2 in Princeton Aeronautical Paperbacks, Princeton University, Princeton NJ, USA. 1960.

Hinanshu Shekhar, ''Estimation of Pressure Index and temperature sensitivity coefficient of solid rocket propellants by static evaluation'', Defence Science Journal, Vol 59, No 6, November 2009.

R.T. Holzmann. Chemical Rockets, Marcel Dekker, New York, NY,USA. 1969.

K.K. Kuo. Non-intrusive combustion Diagnostic, Begell House Inc. New York.1994

A.A. Juhasz. and C.F. Price. ''The Closed Bomb Technique for Burning rate Measurement at High Pressure''. AIAA progress in Astronautics and Aeronautics. 1978, Vol. 63.

C.M. Mihlfelth, A.D. Baer, and N.W. Ryan. ''The Response of Burning Rate Propellant Surface to thermal radiation'', AIAA Journal. 1972.

R. Nakka Solid propellant burn rate, Web.5,Nov, 2013.

National Aeronautics and Space Administration. ''Space Vehicle Design Criteria (chemical propulsion. Solid propellant grain design)''. NASA SP-8076, pp. 28.

G.P. Sutton. Rocket Propulsion Elements, Wiley, New York, USA, 6th Edition. 1992.

L.D. Strand, A.L. Schults and G.K. Reedy. ''Microwave Measurement of Solid propellant Pressure Coupled Response Function'', Journal of Spacecraft and Rockets. 1980, pp. 483-488..

Space Travel Guide, Web, 5 January 2014, <http://library.thinkquest.org/03oct/02144/propulsion/propellents/solidclass.htm>

J.M. Tauzia and P. Lamarque. Solid rocket Propellant Behaviour during Static Firing Test using Real Time X-Ray Radioscopy, paper 35 AGARD, 1998 Paris, France.

The MFC Propulsion Program, Application of Today's Propulsion Technology to Space Commercialization, Web, 10 December 2013, http://www.sps.aero/Propulsion_Program/MFC_Intro.htm

F.A. Williams. Combustion Theory, the Benjamin/Cummings Publishing Company, Menlo Park, CA, 2nd Edition. 1985.

L.C. Yang and E.L Ramanos. '' Application of Plasma Capacitance Gage for Real Time Measurements for Solid Rocket Motor Internal Insulation Erosion'', AIAA Paper, 1990, pp. 90-2327.

C. Zanotti, A. Volpi, M. Bianchessi and L.T. Deluca. Measuring Thermodynamic Properties of Burning Propellants, AIAA Progress in Astronautics and Aeronautics, Non steady burning and combustion stability of solid propellants, edited by Deluca et al, chapter 5, pp. 145-196, AIAA Wishington DC, USA. 1992.

V.E. Zarko and K.K. Kuo ''Critical Review of methods of regression rate measurements of condensed Phase systems'' pp 600-623

Nnali-Uroh, Emmanuel is a staff of Rocket fuel Division, Centre for space Transport and Propulsion Epe, an activity centre of National Space Research and Development Agency (NASRDA).He holds a master degree in Chemical and polymer Engineering from Lagos state University, an Advance Diploma in AeroMech Engineering from Air Force Institute of Technology Kaduna and a B. Tech in Chemical Engineering Ladoke Akintola University of Technology Ogbomoso , Oyo State. His research interest includes Rocket fuel development and combustion analysis, propellant characterization, process analysis and modelling. He is a registered member of Nigerian Society of Engineers (NSE).

Oyedeko Kamilu Folorunsho is a lecturer in the Department of Chemical and Polymer Engineering, Lagos State University, Lagos. He holds a PhD degree in Chemical Engineering from Lagos State University, Lagos and he has graduated many undergraduate and Post graduate students. He has published many journal articles. His research interests include; Process Analysis and Optimization in Chemical Engineering, Thermodynamics, Transport Phenomenon, Petroleum Technology and Reservoir Engineering. He is a Registered Engineer, a member of Nigerian Society of Engineers, is a member of Nigerian Society of Chemical Engineers, and is a member of Society of Petroleum Engineers.